04,12

Influence of carbon black content on the electrophysical characteristics of polymer composites

© A.M. Zyuzin, K.E. Igonchenkova

Ogarev Mordovian State University,
Saransk, Russia

E-mail: zyuzin.am@rambler.ru

Received August 13, 2025
Revised August 20, 2025
Accepted October 21, 2025

A sharp increase in the effective dielectric constant of composites with an ethylene vinyl acetate matrix at carbon black concentrations corresponding to the percolation region has been established, as well as the presence of a maximum dielectric loss at concentration, when the dominant contribution to conductivity is due to field emission. A correlation has been revealed between the dependences of the effective dielectric constant and conductivity on the carbon black content. In composites with a carbon black concentration corresponding to the percolation point and higher, a deviation of the experimental dependence of the capacitor capacity on the sample thickness from the calculated one was found. It is shown that the degree of deviation increases with increasing conductivity and decreasing frequency. At a conductivity value greater than $\sim 2\,\Omega^{-1}\cdot \mathrm{m}^{-1}$, the capacitance of the capacitor ceases to depend on the thickness of the sample. An approach based on the quasi-electrostatic approximation is proposed to explain the results obtained, as well as the high values of the effective dielectric constant of semiconducting materials.

Keywords: effective dielectric constant, polymer composites, carbon black, electrical conductivity.

DOI: 10.61011/PSS.2025.10.62631.230-25

1. Introduction

Polymer composite materials filled with nanoscale electrically conductive particles attract the researchers attention and are of practical interest, since their electrophysical characteristics, such as conductivity, permittivity and loss-angle tangent, may be adjusted within a wide range. The possibility of achieving the required values of these parameters is what drives the use of such materials as effective radiation-absorbing shells, antistatic coatings and etc. [1–5]. A fairly high permittivity coupled with a low level of dielectric losses makes these materials fit for use not only as conductive, but also as electric field refractive materials. Electrophysical properties of composites based on polymers and carbon fillers were studied by many research groups. It was demonstrated that the real part of effective permittivity ε' rises with increasing carbon filler content [6,7]. For example, a rise of ε' with the increasing concentration of carbon black in ethylene propylenediene matrix composite was reported in [7]. This was attributed to the influence of interfacial polarization at the interface between the polymer matrix and filler particles. As was stressed in [8], the Bruggeman approach to calculation of permittivity of a medium with conducting particles is more rigorous than the Maxwell–Garnett one. The calculation of ε' becomes significantly more complicated when the conductive filler particles have a complex and varied shape and when the composite contains both individual particles and their agglomerates. These include polymer composites based on an ethylene vinyl acetate matrix filled with carbon black (CB), which are critical for practical use and, specifically, for fabrication of the HV power cables shields. The purpose of this work was to study the effect of the carbon black content and the electric field frequency on the real part of the effective permittivity ε' and loss-angle tangent $\mathrm{tg}\,\delta$ of composites containing ethylene vinyl acetate matrix. The capacitor method is widely used to determine the complex dielectric constant in materials with a sufficiently large range of conductivity values (method of parallel plates [9–12]. ε' is found from the ratio of the capacitance C_x of a flat capacitor, between the electrodes (plates) of which the studied material is placed, to the capacitance C_0 of an equivalent capacitor, when there's vacuum (air) in the space between the electrodes $\varepsilon' = C_x/C_0 = C_x d/(\varepsilon_0 S)$ [8], where, d — distance between the electrodes, $\varepsilon_0 = 8.85\cdot 10^{-12}$ F/m — electric constant, S — area of electrodes. Impedance spectroscopy also takes into account the thickness of the sample located between the electrodes of the capacitor [12,13]. In this regard, strict compliance with the ratio $C \sim 1/d$ should be considered as one of the criteria for the correctness of using the capacitor method to determine ε', including semi-conducting materials. Therefore, among the tasks of the work was studying the effect of the sample thickness on the capacitance of the flat capacitor at different specific conductivities σ of the material.

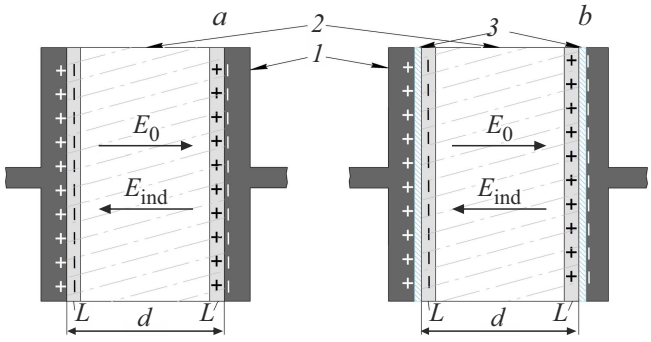

Figure 1. Capacitance measurements diagrams: *a* — variant 1, *b* — variant 2; *1* — electrodes, *2* — sample, *3* — insulating films, L — thickness of induction charges layers, d — sample thickness.

2. Experiment

The experiment used polymer composites based on a matrix of ethylene vinyl acetate (EVA) filled with carbon black grade C40, the particle sizes of which are 20–60 nm [14]. The composite samples were fabricated by mixing the polymer matrix in melt in the laboratory extruder EX30. The plates 1–1.5 mm thick were fabricated further by pressing. The thickness d of the studied samples was changed by changing the number of superimposed discs with a diameter of 20 mm which were cut from the original plates. The carbon black content in the composites ν varied from 5 to 35 wt.%. Depending on ν, specific conductivity varied from $3 \cdot 10^{-9}\,\Omega^{-1}\mathrm{m}^{-1}$ to $2\,\Omega^{-1}\mathrm{m}^{-1}$. The resistivity of high-resistance composites was measured using Megger MIT1025 device, the resistance of low-resistance composites with a carbon black content of $\nu > 20\,\%$, was measured by RIGOL DM3058. The capacitance and loss angle tangent in the frequency range f from 50 Hz to 1 MHz were measured using an immittance meter E7-20 complete with a measuring cell with round electrodes $D = 20$ mm in diameter and 1.5 mm thick. To eliminate the impact of possible uncontrolled air layers, a silver conductive paste was applied. When measuring the capacitance, a pressure of $20\,\mathrm{N/cm}^2$ was applied to the samples from the electrodes. The influence of the edge effects on C was taken into account according to the expression [15]:

$$C = \varepsilon_0 \frac{\pi R^2}{d} + \varepsilon_0 R \left(\ln \frac{16\pi R}{d} - 1 \right),$$

where R — radius of electrodes, and the value $\varepsilon_0 R \left(\ln \frac{16\pi R}{d} - 1 \right)$ — correction due to the edge effect. The parasitic capacitance of the measuring cell and the supply conductors was also taken into account, which was 1.8 pF. It is hard to determine the permittivity of semiconducting materials, especially when reach-through conductivity occurs in the sample. We applied the following capacitance measurement schemes (Figure 1): first variant — in direct contact of electrodes with the sample; second variant: thin insulating films of polyethylene terephthalate 15 μm thick were placed between the sample and each of the capacitor electrodes to remove the effect of the reach-through conductivity current; in the third variant, two similar films folded together were placed only on one side of the sample [16]. A similar arrangement is found in operation of a composite shield of HV cable located between the conductor and the insulating layer.

The capacitance of a capacitor with a sample and insulating films C_e can be considered as the capacitance of two capacitors connected in series: 1) a capacitor containing only the test sample tightly adjacent to the electrodes, with a capacitance of C_x; 2) a capacitor containing only two films and difficult-to-control air layers, with a capacitance of C_i. Such interlayers may introduce significant errors into the measurement results [10] (especially the results for thin samples or samples with high permittivity ε'. For this system the ratio may be written

$$\frac{1}{C_e} = \frac{1}{C_x} + \frac{1}{C_i},$$

which yields

$$C_x = C_e \left(1 + \frac{C_e}{C_i - C_e} \right).$$

The values ε' were found as $\varepsilon' = C_x d/(\varepsilon_0 S)$.

3. Results and their discussion

3.1. The effect of the carbon black content on the effective permittivity and the loss-angle tangent

Figure 2 shows the obtained dependences of effective permittivity ε' on carbon black content at frequency levels 50 Hz and 1 MHz. Note that since, as will be shown below, for concentrations of CB $\nu > 15\,\%$, there is a deviation of the experimental dependence of capacitance on the sample thickness from the calculated value, the value ε' was determined for the case of the minimum samples thickness (1–1.2 mm). In the first variant of measurements with the rise of ν from 0 to 35 % the capacitance grew from 7.2 to 11400 pF at 50 Hz and to 1570 pF at a frequency of 1 MHz.

It follows from the presented results that the $\varepsilon'(\nu)$ dependence has an initial section with a shallow slope in the region of low concentrations, whereas the values ε' being practically independent of the measurement variant. In the percolation region, i. e. with the concentrations of CB 15–25 %, a drastic rise of ε' occurs, then, at $\nu > 25\,\%$ the rise of ε' with the growing ν becomes lower again. A similar dependence of $\varepsilon'(\nu)$ was observed in the entire studied frequency range from 50 Hz to 1 MHz. Calculations of the dependence of effective permittivity on concentration $\varepsilon'(\nu)$ based on both the Maxwell–Garnett approach and the

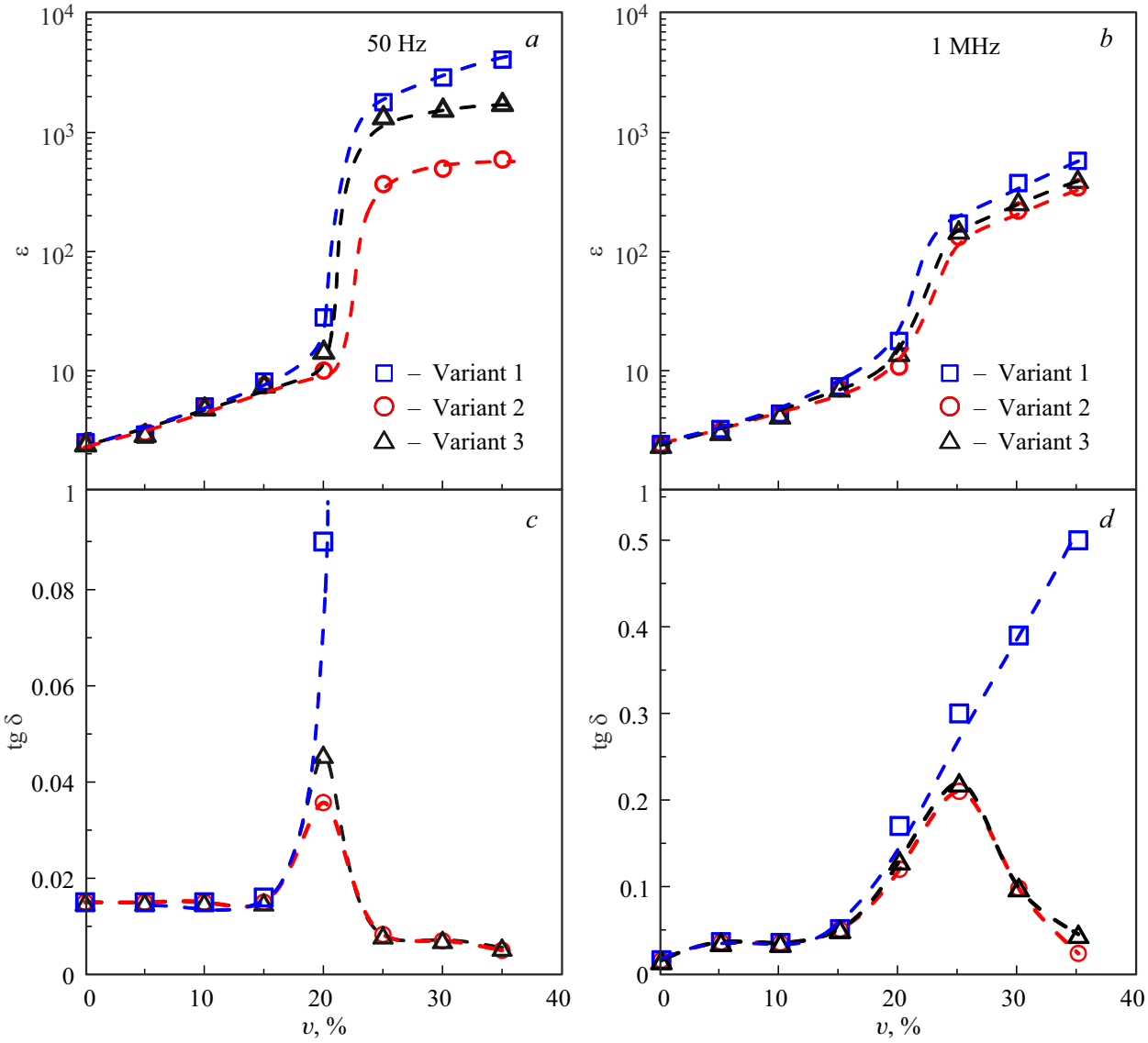

Figure 2. Effective permittivity ε' (a, b) and loss-angle tangent $\mathrm{tg}\,\delta$ (c, d) at 50 Hz (in the left) and 1 MHz (in the right) versus concentration of carbon black v for various measurement variants.

Bruggeman approach do not provide satisfactory agreement with the experimental data.

Figure 3 shows the dependence of conductivity on the concentration of carbon black. It follows from the comparison of dependences $\varepsilon'(v)$ and $\sigma(v)$ shown in Figures 2 and 3 that they are correlated qualitatively. Experimental dependence $\sigma(v)$ agrees fairly closely with the one calculated according to the following expressions [1]

$$\sigma_1 = (v - v_c)^t, \quad \text{by} \quad v > v_c$$

$$\sigma_2 = (v_c - v)^{-s}, \quad \text{by} \quad v < v_c,$$

following from the classical percolation theory, where v_c is the critical concentration, which was 17 %, and t and s are the critical indices, which in this case are 4 and 1.5 accordingly.

The dependence of the dielectric loss-angle tangent $\mathrm{tg}\,\delta$ on the carbon black content differs significantly from the dependence $\varepsilon'(v)$ and has a non-monotonic character in the measurement variants 2 and 3 (Figure 2 *c, d*). At 50 Hz, at a concentration of $v = 20$ % corresponding to the percolation region (15–25 %), the increase of $\mathrm{tg}\,\delta$ and a peak are observed. As follows from Figure 2, at a frequency of 1 MHz, a peak of $\mathrm{tg}\,\delta$ is also observed, but its position is displaced towards the region of high concentrations of CB ($v = 25$ %). This behavior $\mathrm{tg}\,\delta(v)$ was reproduced on three series of samples. In addition, we observed a similar behavior of the dependence $\mathrm{tg}\,\delta(v)$ and the presence of a maximum at $v = 15$ % in EVA-based composites filled with carbon black P267E, which has a higher dispersion and provides slightly higher conductivity and a lower percolation threshold at the same concentrations with C40.

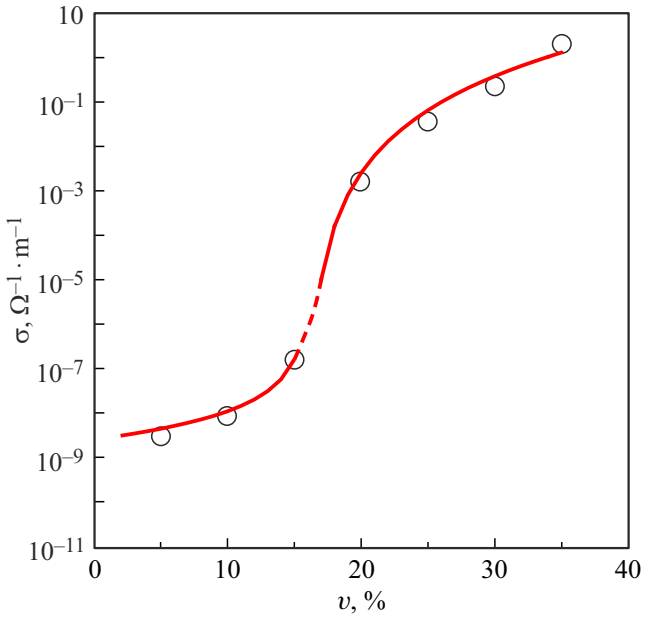

Figure 3. Specific conductivity of the composite versus CB concentration (C40), circles — experiment, solid sections of line — calculated.

One of the possible mechanisms behind the observed increase in losses and appearance of peak at $\mathrm{tg}\,\delta$ is related to the fact that at concentration of $\nu \geq 15\,\%$ the conductivity rises significantly at such concentrations and the conductivity component induced by field emission of electrons from the surface of carbon black particles with subsequent tunneling becomes dominant. This, in turn, may be associated with certain specific features of energy dissipation processes leading to an increase in losses. Field emission is characterized by a nonlinear current-voltage curve specified by the Fowler–Nordheim relation [17], which agrees with the experimental data for the sample with $\nu = 20\,\%$. Note that the presence of a peak on the concentration dependence of $\mathrm{tg}\,\delta$ for composites based on oligomeric di-isocyanate filled with barium titanate particles ($BaTiO_3$) was also observed in the study [18]. For larger ν, the values $\mathrm{tg}\,\delta$ in the measurement variant 1 were by 1–2 orders higher compared to variants 2 and 3, which can be explained by the influence of the reach-through conductivity current, the oscillation phase of which, unlike the capacitive component of the current coincides with the voltage phase.

Figure 4 shows the obtained dependences of effective permittivity and $\mathrm{tg}\,\delta$ on the frequency for three composites with different values ν. It can be seen that with increasing frequency, there is a monotonous decrease in the values of both ε' and $\mathrm{tg}\,\delta$, which is especially pronounced in composites with a high content of carbon black.

One of the interesting findings is the discovery of dependence of ε' on the measurement variant. If at low concentrations there is practically no noticeable difference in the values of C_e, and therefore ε', then starting from the concentration of carbon black $\nu = 15\,\%$ and higher, this difference becomes very noticeable, especially at low measurement frequencies. The slightly higher values of ε' in variants 1 and 3 can be explained by the rising effect on C_x of the charge in the sample's near-surface layer resulting from the injection of electrons from the electrode(s) in contact with the sample without any insulating layer.

3.2. Influence of conductivity on electrical capacitance versus sample thickness

The findings from the study of influence of composites samples thickness with different amount of electric con-

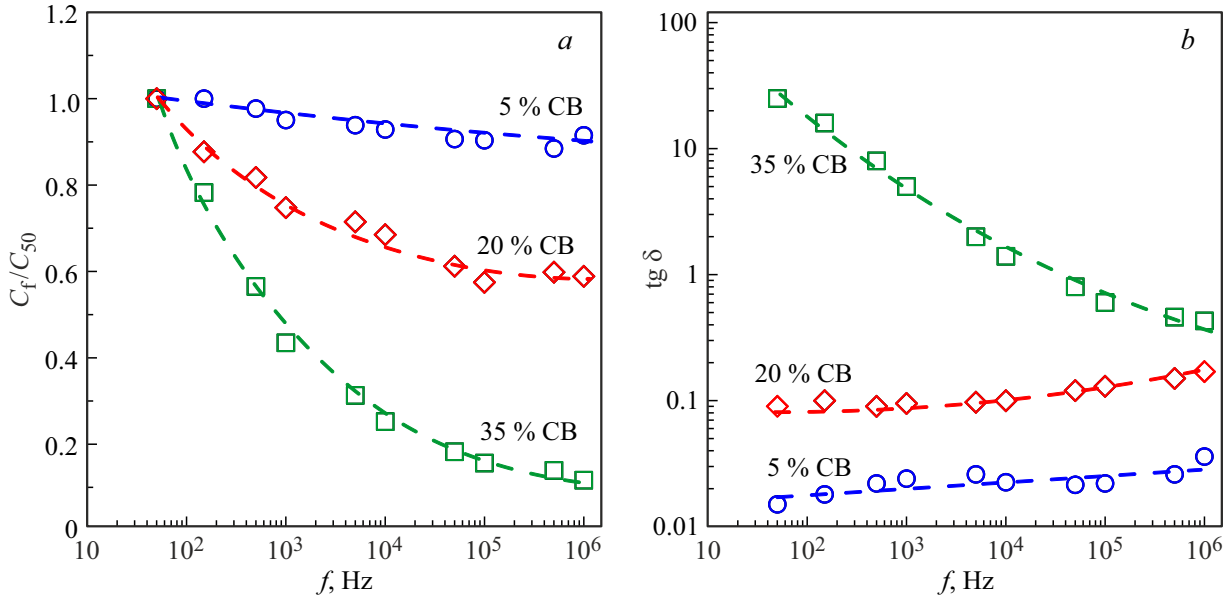

Figure 4. Capacitance (a) and loss-angle tangent (b) versus frequency in composites with various content of carbon black.

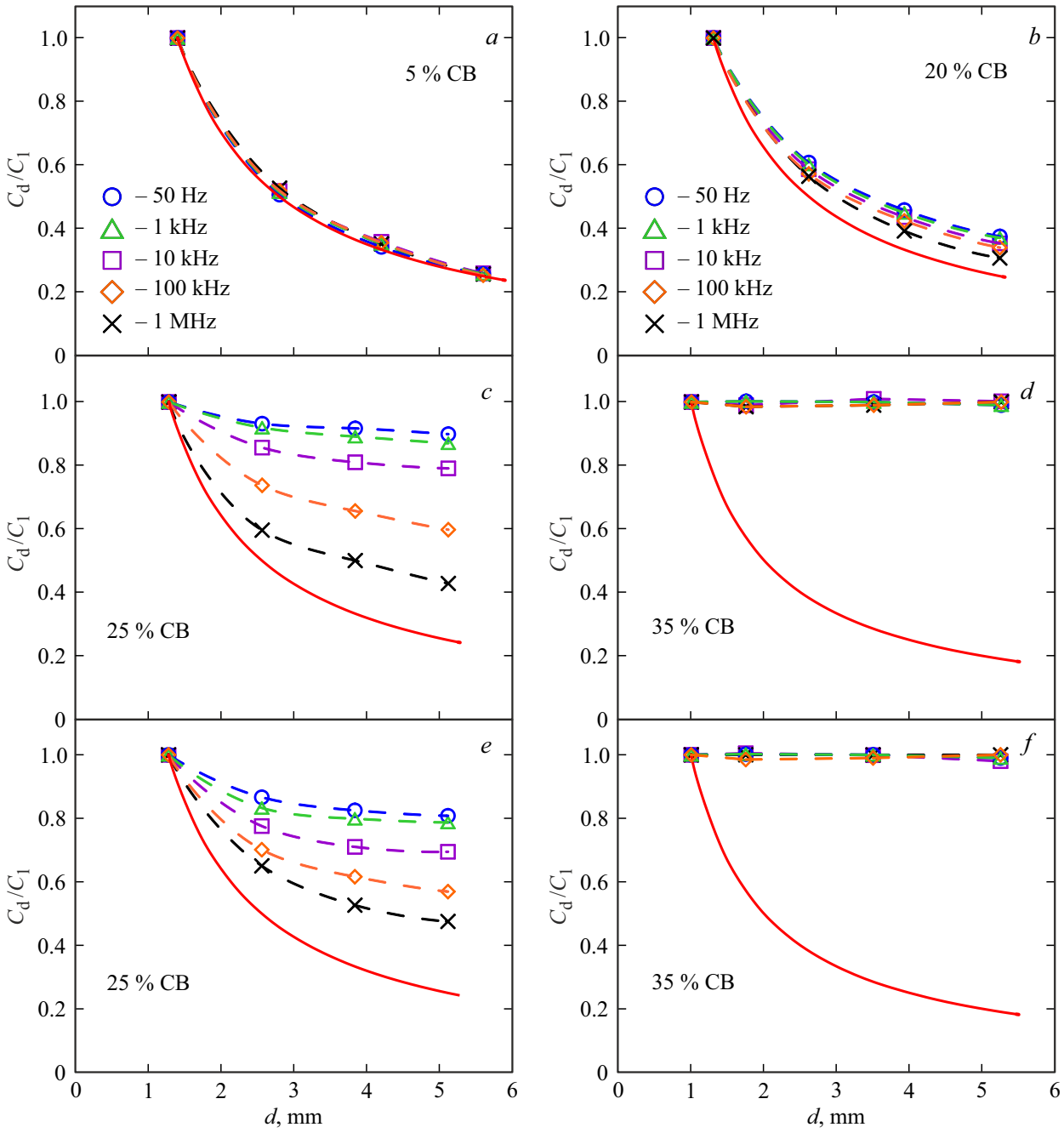

Figure 5. Experimental (symbols) and calculated (solid lines) dependences of the normalized capacitances C_d/C_1 on the thickness of composite samples with different content of carbon black ν: $a-d$ — variant 1, e,f — variant 2.

ducting filler and, respectively, having various values of specific conductivity σ on the capacitance are provided in Figure 5, $a-d$ (variant 1) and e,f (variant 2). Both, for the original ethylene vinyl acetate matrix ($\nu = 0$), and for composites with black carbon content of $\nu = 5-15\,\%$, for which conductivity σ varied from 10^{-9} to $10^{-7}\,\Omega^{-1}\mathrm{m}^{-1}$, the experimental dependencies of capacitance on the samples thickness on all studied frequencies obey the law $C_d/C_1 \sim 1/d$, where C_1 — capacitance at minimal sample thickness.

Then, as follows from Figure 5, b, when the carbon black content $\nu = 20\,\%$ ($\sigma \approx 10^{-3}\,\Omega^{-1}\mathrm{m}^{-1}$), the experimental ratio C_d/C_1 starts greatly diverge from the calculated one. In composites with $\nu = 25\,\%$, for which $\sigma \approx 4 \cdot 10^{-2}\,\Omega^{-1}\mathrm{m}^{-1}$, this divergence becomes even more pronounced. We may see that divergence depends on the frequency f and declines with the frequency growth. At $\nu = 30\,\%$ of CB ($\sigma \approx 2 \cdot 10^{-1}\,\mathrm{m}^{-1}$) the experimental dependencies C_d/C_1 at different frequencies had even a more pronounced divergence from the calculated one. And

finally, in composites with $\nu = 35\,\%$ of CB, for which the conductivity makes about $2\,\Omega^{-1}\mathrm{m}^{-1}$, the capacitance in the studied range of values d ($1\,\mathrm{mm} < d < 6\,\mathrm{mm}$) stops depending on the sample thickness. We observed a similar behavior of the dependence C_d/C_1 in EVA-based composites filled with carbon black P267E, which, as noted above, has a higher dispersion and provides slightly higher conductivity and a lower percolation threshold at the same concentrations with C40. For such composites a distinct deviation of dependence C_d/C_1 from the calculated one started already at $\nu = 15\,\%$, and at 30 % of CB the capacitance stopped being dependent on d. As follows from the experimental results, the presence of two insulating films in the measurement variants 2 (Figure 5, *e,f*) and 3 did not qualitatively affect the behavior of the dependencies C_d/C_1 on the thickness of the samples.

The observed deviations of the dependencies C_d/C_1 from the calculated ones can be explained as follows. The capacitance of a flat capacitor with a sample filling the entire space between the electrodes is defined as $C = \varepsilon'\varepsilon_0 S/d$, i. e., in addition to the geometry S and d, it also depends on the effective permittivity. An increase in the capacitance in the presence of a dielectric corresponds to a greater ability to retain a free electric charge on the plates and is caused by the electric field of polarizing (bound) charges of the opposite sign that occur in the thin near-surface layers of the dielectric. With the content of CB in the composite $\nu = 5-10\,\%$ and even low conductivity, the Maxwell–Wagner [19] interfacial polarization begins to have a noticeable effect on the values of ε related to the dipole moments of isolated conductive CB particles arising under the action of a field. With a further increase of ν and, as a result, a rather sharp increase in the conductivity in the percolation region of [3], the dominant effect on the magnitude of the resulting field in the sample, and consequently on the values of C and ε' begin to exert induction charges formed in the near-surface layers of the sample due to electrostatic induction and the process of establishing electrostatic equilibrium. In the presence of ohmic contact, charges with a certain volume density of ρ injected from the electrodes into the near-surface region(s) of the sample under the field action can have an additional effect. The behavior of such charges is described by the time of Maxwellian relaxation τ_m, that can be found based on the charge conservation law $\mathrm{div}\,\mathbf{j} = -\frac{\partial \rho}{\partial t}$, Ohm's law $\mathbf{j} = \sigma\mathbf{E}$ and Gaussian theorem $\mathrm{div}(\varepsilon'\varepsilon_0\mathbf{E}) = \rho$ in the differential form [20,21]. As a result, we obtain an equation describing the dynamics of changes in charge density $\rho(t) = \rho_0 e^{-\frac{t}{\tau_m}}$, where $\tau_m = \varepsilon'\varepsilon_0/\sigma$ — time of Maxwellian relaxation. As noted in [20,21], due to the interaction of electrons with the lattice ions and due to inertia, the charge relaxation time, e.g., in metals is about 3–4 orders of magnitude higher than the values calculated according to the above expression for τ_m.

The electrostatic equilibrium in a sample located between the capacitor electrodes, including in the presence of insulating films, is provided because of shifting the array of free charges (current) in the initially electrically neutral (equilibrium) medium of the sample due to the drift motion of charges in the resulting electric field $E_1 = E_0 - E_{ind}$, where E_0 — the field created by charges on the capacitor electrodes, and E_{ind} —the induction field created by two near-surface layers of dissimilar induction charges in the sample (Figure 1). Note that when exposed to alternating voltage, the oscillation phase of the above current coincides with the phase of the electrodes charging current and outpaces the phase of voltage fluctuations and, accordingly, the phase of the reach-through conductivity current by $\pi/2$. The field of induction charges will strive to the value of external field E_0, while the resulting field E_1 will go to zero. At a certain value of conductivity, the degree of E_1 approximation to zero (achieving electrostatic equilibrium) will not depend on the thickness of the sample located between the electrodes of the capacitor. This is fundamentally different from the non-conducting dielectric material, in which the field of polarization charges $E_p = E_0(\varepsilon' - 1)/\varepsilon'$, and the resulting field $E_1 = E_0/\varepsilon' = U/(\varepsilon' d)$, where U — is the applied voltage.

Let us consider the establishment of an electrostatic equilibrium in a semi-conducting sample located between the electrodes of a capacitor, based on the quasi-electrostatic approximation [20–22]. Thus, the resulting field E_1 in the sample

$$E_1 = E_0 - E_{ind}, \tag{1}$$

where

$$E_{ind} = \frac{enL}{\varepsilon'\varepsilon_0'}, \tag{2}$$

enL — induction charge per unit of the sample surface area, n — concentration of free charges (conductivity electrons), L — time-dependent thickness of positive and negative charged layers (Figure 1), occurring as a result of the drift motion of electrons in the field E_1. Then, $L \ll d$ will be defined by the expression:

$$L = \int_0^t \upsilon dt, \tag{3}$$

where υ — average drift velocity of electrons. In permanent field E_0 this velocity is constant: $\upsilon = (eE_0\tau_*)/(2m_*)$ [22], where e and m_* charge and effective mass of the electron, respectively, τ_* — average time between two consecutive collisions of electrons with the lattice ions ($\tau_* \ll t$). But since the motion of electrons does not occur in a permanent field, but in a changing resultant field E_1, their acceleration, and therefore the average velocity they acquire over time τ_*, will also depend on time:

$$\upsilon = \frac{eE_1}{2m_*}\tau_*. \tag{4}$$

Inserting (4) into (3), we obtain

$$L = \frac{e\tau_*}{2m_*}\int_0^t E_1 dt. \tag{5}$$

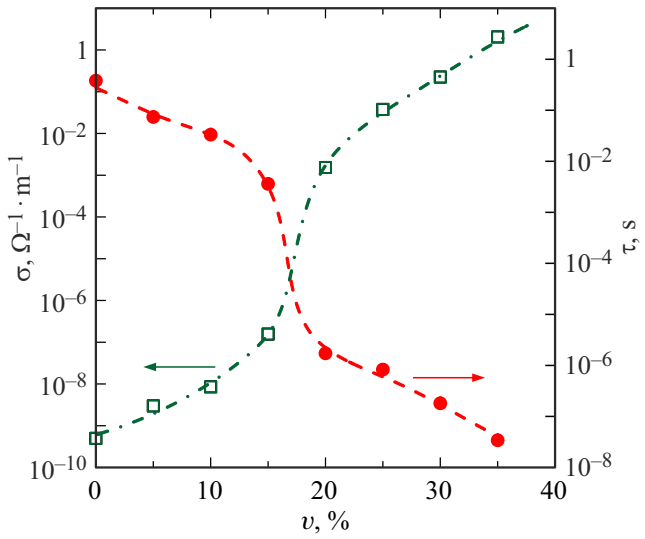

Figure 6. Time of setting the electrostatic equilibrium τ and the specific conductivity σ versus carbon black content in composites.

From the expressions (2) and (1) it follows:

$$E_1 = E_0 - \frac{ne^2\tau_*}{2m_*\varepsilon'\varepsilon_0}\int_0^t E_1 dt = E_0 - \frac{\sigma}{\varepsilon'\varepsilon_0}\int_0^t E_1 dt, \qquad (6)$$

where $\sigma = (ne^2\tau_*)/(2m_*)$ — specific conductivity. Differentiating (6) with respect to time, we obtain:

$$\frac{dE_1}{dt} = -\frac{\sigma}{\varepsilon'\varepsilon_0}\frac{d}{dt}\int_0^t E_1 dt. \qquad (7)$$

According to Barrow's theorem, the derivative of a certain integral with a variable upper limit is equal to the value of the integral function at this limit. Therefore, equation (7) can be written as:

$$\frac{dE_1}{dt} = -\frac{\sigma}{\varepsilon\varepsilon_0'}E_1. \qquad (8)$$

After integration of this equation, having taken $E_1 = E_0$ as initial value, and E' as final value we obtain for the time τ which will be the time needed to achieve this value E' or at $E' \ll E_0$ — time to achieve the electrostatic equilibrium:

$$\tau = \left(\ln\frac{E_0}{E'}\right)\frac{\varepsilon'\varepsilon_0}{\sigma}. \qquad (9)$$

Figure 6 illustrates the conductivity σ and time τ versus carbon black content v, as found from (9) based on the appropriate values of conductivity σ at $E' = 10^{-3}E_0$. It can be seen that for materials with low conductivity $\sigma < 10^{-8}\,\Omega^{-1}\mathrm{m}^{-1}$, the time to establish the equilibrium state is > 0.05 s. Therefore, even at low frequencies of the electric field ($f = 50$ Hz), electrostatic equilibrium will not be achieved, and this factor will not have any great effect on C and ε', and, consequently, on the divergence of the capacitance versus sample thickness from the calculated dependence.

That is, when the time for setting the electrostatic equilibrium τ is high compared to $1/\omega = 1/(2\pi f)$, or $\omega\tau \gg 1$, the ratio $C_d \sim 1/d$ is fulfilled. When, in its turn, τ becomes comparable with $1/\omega$ ($\omega\tau \approx 1$), then, though some dependence of C on d still exists, it starts to diverge from the calculated values. This explains the dependence of the divergence on frequency — the higher the frequency, the smaller the deviation of the dependence $C(d)/C_1$ from the calculated values. And, finally, when time τ becomes much less $1/\omega$ ($\omega\tau \ll 1$), the capacitance of the capacitor with the sample stops being dependent on thickness d. The influence of induction electric charges arising in the near-surface layers of the sample can also explain the high values of the effective dielectric constant of semi-conducting materials observed with the rise of conductivity. These charges with their influence explain high surface charge density on the capacitor electrodes, which leads to high values of C and, accordingly, ε'.

4. Conclusion

Based on the results obtained in the present study, the following conclusions can be made.

1. It was found that the effective permittivity of a composite with an ethylene vinyl acetate matrix increases sharply at carbon black concentrations corresponding to the percolation region. With the rise of conductivity, the dominant factor determining the capacitance and, consequently, the effective dielectric constant becomes the induction charges that arise in the near-surface layers of the sample due to electrostatic induction and the establishment of electrostatic equilibrium. The concentration dependences of permittivity and conductivity of composites are correlated qualitatively.

2. The maximum dielectric loss observed near the percolation point can be explained by the fact that at such a concentration the contribution to conductivity due to the field emission of electrons from the surface of carbon black particles with subsequent tunneling becomes dominant. This, in turn, is associated with certain specific features of energy dissipation processes leading to higher losses.

3. A deviation of the experimental dependence of the capacitance on the thickness of semi-conducting samples from the calculated values was found. The magnitude of the deviation increases with the growth of conductivity and lower frequency of the electric field. Higher values of $C(d)/C_1$ at a lower frequency are due to a greater degree of compensation of the electric field induced by the electrodes' charges, field of induction charges.

4. It was found that when conductivity $\sigma \approx 2\,\Omega^{-1}\mathrm{m}^{-1}$ is reached, the capacitance of the capacitor with the sample stops being dependent on the sample thickness. The influence of the discovered features of the experimental

dependence $C(d)$ of semi-conducting materials can lead to significant inaccuracies in the determination of ε' and incorrect interpretation of the results.

5. An approach based on a quasi-electrostatic model is proposed, which makes it possible to calculate the time for setting the electrostatic equilibrium and explains the observed deviations of experimental dependences $C(d)$ from calculated ones, as well as large values of the effective permittivity of semiconducting materials.

Conflict of interest

The authors declare that they have no conflict of interest.

References

[1] E.R. Blythe, D. Bloor. Elektricheskie svoistva polymerov. Fizmatlit, M. (2008). 378 p. (in Russian).
[2] V.A. Markov, V.A. Gushchin, A.V. Markov. Plasticheskie massy **1**–**2**, 44 (2019).
[3] A.M. Zyuzin, A.A. Karpeev, N.V. Yantsen. ZhTF **92**, *6*, 829 (2022). (in Russian).
[4] A.S. Stepashkina, E.S. Tsobkallo, O.A. Moskalyuk, A.N. Aleshin. Pis'ma v ZhTF **41**, *2*, 7 (2015). (in Russian).
[5] W. Li, U.W. Gedde, H. Hilborg. IEEE Trans. Dielectr. Electr. Insul. **23**, *2*, 1156 (2016).
[6] I.A. Markevich, G.E. Selyutin, N.A. Drokin, A.G. Selyutin. ZhTF **90**, *7*, 1151 (2020).
[7] M. Rahaman. RSC Adv. **13**, *36*, 25443 (2023).
[8] B.A. Belyayev, V.V. Tyurnev. ZhETF **154**, *4*, 716 (2018). (in Russian).
[9] A. Ameli, M. Nofar, C.B. Park, P. Potschke, G. Rizvi. Carbon **71**, 206 (2014).
[10] V.A. Akzigitov, A.A. Belyaev, A.O. Kurnosov, S.M. Payarel', Tr. VIAM, **132**, *2*, 12 (2024). (in Russian).
[11] Y. Hazama, N. Ainoya, J. Nakamura, A. Natori. Phys. Review B **82**, *4*, 045204 (2010).
[12] V.G. Pleshchev. FTT **65**, *5*, 767 (2023). (in Russian).
[13] A.V. Ilinskiy, R.A. Kastro, A.A. Kononov, M.E. Pashkevich, E.B. Shadrin. FTT **65**, *8*, 1325 (2023). (in Russian).
[14] G.V. Moiseevskaya, G.I. Razd'yakonova, M.Yu. Karavaev, A.A. Petin, E.A. Strizhak. Kauch. Rezina, *4*, 24 (2015). (in Russian).
[15] L.D. Landau, E.M. Lifshits. Elektrodinamika sploshnykh sred. Fizmatlit, M. (2005). 656 p. (in Russian).
[16] A.M. Zyuzin, K.E. Igonchenkova, A.A. Karpeev. PZhTF **51**, *10*, 40 (2025).
[17] A.M. Zyuzin, A.A. Karpeev, K.E. Ignchenkova. PZhTF **49**, *13*, 21 (2023).
[18] V. Myakin, N.A. Bubis, L.M. Kuznetsov, M.V. Zhukov, A.Yu. Shmykov. FTT **64**, *6*, 746 (2022). (in Russian).
[19] V.A. Sotskov. ZhTF **83**, *10*, 85, (2013). (in Russian).
[20] V.I. Yakovlev. Classicheskay elektrodinamika. University of Novosibirsk, Novosibirsk (2003). 267 p. (in Russian).
[21] A. Zangwill. Modern Electrodynamics. Cambridge Press, Cambridge (2012). 998 p.
[22] V.A. Aleshkevich. Electromagnetism. Fizmatlit, M. (2014). 404 p. (in Russian).

Translated by T.Zorina